

Małgorzata Słota-Valim

*Oil and Gas Institute – National Research Institute*

## Static and dynamic elastic properties, the cause of the difference and conversion methods – case study

In this study the characteristics of elastic parameters of the lower Paleozoic shale formation is presented. Dynamic elastic properties are calculated based on available seismic data calibrated with elastic properties obtained from well logging. Comparison between dynamic and static elastic properties is conducted and the cause of observed difference is discussed. Finally, methods for conversion of dynamic to static elastic properties is presented. Detailed characterization of the shale formation helps highlight which zones are more susceptible to hydraulic fracturing while conversion of dynamic to static elastic properties is performed for further geomechanical modeling purposes and allow more advanced mechanical analysis of unconventional reservoir object.

Key words: shale formation, elastic properties, Young's modulus, Poisson's ratio, Shear modulus, Bulk modulus, hydraulic fracturing.

### Statyczne i dynamiczne parametry sprężyste, fizyczna przyczyna obserwowanej różnicy i propozycja przeliczenia na przykładzie polskich formacji łupkowych

Dokładne rozpoznanie cech obiektu złożowego to podstawowy warunek, którego spełnienie owocuje trafnym wyznaczeniem lokalizacji wiercenia, projektem otworu wiertniczego i jego uzbrojeniem, a także planem efektywnych zabiegów udostępniania złoża węglowodorów. Z punktu widzenia eksploracji złóż typu niekonwencjonalnego, które od paru lat stały się tematem intensywnych badań również i w Polsce, spośród wymienionych wyżej etapów rozpoznania obiektu szczególnie istotny jest projekt otworu, a zwłaszcza jego poziomy odcinek oraz plan zabiegów udostępniania złoża. Niejednorodność formacji gazonośnej na horyzontalnym odcinku otworu, wzdłuż którego planowane są zabiegi szczelinowania hydraulicznego, nakazuje dokładne rozpoznanie ośrodka skalnego. Jego brak pociąga za sobą konsekwencje, gdyż niewłaściwe rozmieszczenie poszczególnych sektorów poddawanych kolejno zabiegom szczelinowania może przyczynić się do nachodzenia na siebie stref zecerpania gazu, co z kolei skutkuje niską lub zerową produkcją. W artykule przedstawiono charakterystykę parametrów elastycznych formacji łupkowej dolnego Paleozoiku, która pozwoliła na wytypowanie stref bardziej podatnych na zabieg szczelinowania hydraulicznego.

Słowa kluczowe: formacja łupkowa, parametry sprężyste, moduł Younga, współczynnik Poissona, moduł sprężystości poprzecznej, moduł sprężystości objętościowej, szczelinowanie hydrauliczne.

### Introduction

Efficient production of hydrocarbons from geological formations of near-zero permeability became a standard throughout the world. It is possible thanks to the use of boreholes with horizontal sections, which are divided into intervals (stages) subjected to hydraulic fracturing treatment. This technique aims to expand preexisting natural fractures and/or develop artificial fracture network, which becomes a path to the wellbore zone for previously trapped gas.

Accurate characterization of unconventional reservoir object is required for optimal well placement, design as well as effective stimulation of gas bearing shale formation.

From the unconventional reservoir exploration point of view, which from few years has become the subject of intense research also in Poland [4], the choice of direction of horizontal section and the design of hydraulic fracturing is especially important.

Commonly observed heterogeneity in shale formations strongly suggests proper recognition of elastic properties of the formation prior to hydraulic fracturing treatment,

as they control rock susceptibility to the treatment and in consequence may help in selection of zones more prone to fracking.

### Elastic properties of rock

In rock mechanics, there are several commonly used elastic parameters, assuming homogeneity of geological formation. These parameters describe behavior of the material including its susceptibility to deformation and failure under applied stress of certain magnitude. The most commonly used elastic properties in solid mechanics are Young modulus ( $E$ ), Poisson's ration ( $\nu$ ), bulk modulus ( $K$ ) and shear modulus ( $G$ ).

Young modulus ( $E$ ) expresses the linear relationship between applied stress ( $\sigma$ ) and associated deformation ( $\varepsilon$ ) [11] (1).

$$E = \sigma / \varepsilon \quad (1)$$

The magnitude of Young modulus can be determined based on compression test results in static conditions. In case of well log or seismic data availability, elastic parameters can be calculated from shear ( $v_s$ ), compressional ( $v_p$ ) waves velocity and bulk density ( $\rho$ ) measured during acoustic logging in the well or seismic survey [1, 7, 10].

Poisson's ratio ( $\nu$ ) is defined by negative ratio of transverse strain ( $\varepsilon_{trans}$ ) to axial strain ( $\varepsilon_{axial}$ ) (2).

$$\nu = -d \varepsilon_{trans} / d \varepsilon_{axial} \quad (2)$$

Strain is negative in case the deformation is stretching which results from axial tension. If the material is subjected to axial compression, it deforms via contraction and the strain is positive.

Poisson's ratio often is used to express the plasticity of rock formation.

Another frequently used parameter is shear modulus ( $G$ ), also known as the modulus of rigidity. It is determined by ratio of shear stress [ $\tau = F/A$ ] to shear strain ( $\varepsilon_{shear} = \Delta x/l$ ), where  $\Delta x$  is transverse displacement and  $l$  stands for initial length (3).

$$G = [F/A] / [\Delta x/l] \quad (3)$$

Shear modulus describes the response of material to shear stress [5].

Finally bulk modulus ( $K$ ) expresses the resistance of material to isotropic volume change ( $\Delta V$ ) when subjected to isometric compression ( $P$ ) i.e. uniform in every direction (4).

$$K = \Delta P / [\Delta V/V] \quad (4)$$

This parameter describes the extent of volumetric deformation of rock as a result of stress acting on it. The inverse of bulk modulus  $K^{-1}$  is known as compressibility [5].

All mentioned above parameters, with the exception of dimensionless Poisson's ratio, are expressed in units of pressure i.e. Pa, bar or psi (1 Pa =  $10^{-5}$  bar = 10.45037738 psi).

Other elastic parameters characterizing the mechanical behavior of geological medium so called Lamé parameters: Lamé's constant ( $\lambda$ ) and Lamé's coefficient ( $\mu$ ) have narrower application in geomechanical modeling and are limited to specific cases [2, 9].

### Elastic parameters of Shale Formation SF1

The object of the study is shale formation of the lower Paleozoic SF. Due to confidentiality reasons the location and other details regarding geological setting must remain private.

Calculation of elastic parameters were performed on seismic data volume SF 3D, which is the property of the project investor. Elastic properties such as Young modulus ( $E$ ), Poisson ration ( $\nu$ ), shear modulus ( $G$ ) and bulk modulus ( $K$ ) were calculated within the boundary of seismic volume covering analyzed shale formation SF 3D. Prior to calculations of elastic properties, the seismic data volume has been subjected to simultaneous inversion (performed by third party) – processing allowing for solving bulk density ( $\rho$ ), compressional ( $V_p$ ) and shear wave velocity ( $V_s$ ) seismic volume. Compressional, shear wave velocity and bulk density cubes were then used to

calculate elastic properties according to the relations known from the literature (5–8) [6, 10]:

$$\nu_{dyn} = v_p^2 - v_s^2 / 2 (v_p^2 - v_s^2) \quad (5)$$

$$E_{dyn} = \rho v_s^2 [(3v_p^2 - 4 v_s^2) / (v_p^2 - v_s^2)] \quad (6)$$

$$G_{dyn} = E/2 + 2\nu \quad (7)$$

$$K_{dyn} = E/3 (1 - 2\nu) \quad (8)$$

where:

- $\nu_{dyn}$  – dynamic Poisson ratio,
- $E_{dyn}$  – dynamic Young modulus,
- $G_{dyn}$  – dynamic shear modulus,
- $K_{dyn}$  – dynamic bulk modulus,
- $v_p$  – compressional wave velocity,
- $v_s$  – shear wave velocity,
- $\rho$  – bulk density.

The calculation of elastic properties were performed in six intervals distinguished based on total organic carbon (TOC) content criteria. Due to the confidential character of the data the results will be presented with the limitation to the one of six intervals – shale formation (SF1).

The summary of statistical parameters and distribution of particular elastic property i.e. Young modulus ( $E$ ), Poisson's ratio ( $\nu$ ), bulk modulus ( $K$ ) and shear modulus ( $G$ ) describing SF1 formation are showed in Table 1.

**Statistical characteristics**

Histograms of analyzed mechanical parameters: Young's modulus ( $E$ ), Poisson's ratio ( $\nu$ ), bulk modulus ( $K$ ) and shear modulus ( $G$ ) made for interval SF1 have leptokurtic distribution which indicates strong clusterization of samples, resulting in higher peak (higher kurtosis) around the center of distribution – distribution mean. In addition, the distribution of Poisson's ratio ( $\nu$ ) and bulk modulus ( $K$ ) displays asymmetry, in case of Poisson's ratio right-skewed distribution

Table 1. Statistical parameters of selected elastic properties of Shale Formation SF1 with histograms made for Young modulus ( $E$ ), Poisson's ratio ( $\nu$ ), bulk modulus ( $K$ ) and shear modulus ( $G$ )

Elastic properties calculated for SF1	Range of value	Distribution mean	Histogram
Young modulus ( $E$ ) [GPa]	0÷51.56	31.70 42.32	
Poisson's ratio ( $\nu$ )	0÷0.347	0.274 0.317	
Bulk modulus ( $K$ ) [GPa]	0÷36.95	31.41	
Shear modulus ( $G$ ) [GPa]	0÷20.88	12.10 16.81	

and bulk modulus left-skewed distribution. It indicates high density of samples lower in value than the distribution mean (0.274) in case of Poisson's ratio distribution and in case of the distribution of bulk modulus higher than the mean equal to 31.41 GPa.

In case of Young modulus ( $E$ ) and shear modulus ( $G$ ) the distribution is bimodal indicating the existence of two sub-facies within analyzed interval SF1, revealing different stiffness and resistance to shear deformation. First sub-facies, lying deeper with the respect to the other one, of higher representation of samples with the mean distribution of Young's modulus equals to 42.32 GPa and shear modulus equals to 16.81 GPa, is stiffer and more resistant to shear strain. The second lying more shallow sub-facies with the distribution means equal to 31.7 GPa and 12.1 GPa for Young's modulus and shear modulus respectively, is less rigid and more susceptible to shear deformation. Among analyzed parameters Young's modulus and Poisson's ratio provide the information whether the given rock formation will frack easily. The distribution of both parameters are slightly mirrored showing that the more representative

sub-facies of higher stiffness and lower plasticity should be more prone to hydraulic fracturing.

From hydraulic fracturing design point of view the intervals subjected to the treatment should reveal susceptibility to generation of artificial fracture networks when sufficient fluid pressure is applied. To be able to determine the areas more prone to fracturing, maps of analyzed interval SF1 showing spatial distribution of elastic parameters were constructed. Maps of average values of Young modulus ( $E$ ), Poisson ratio ( $\nu$ ), bulk modulus ( $K$ ) and shear modulus ( $G$ ) in SF1 interval are presented on Fig. 1–4 respectively.

Spatial distribution of elastic parameters shows that shales of lowest resistance to volume change are localized in southern part of the characterized object, particularly in SE part. Taking into account spatial distribution of Poisson's ration and Young modulus for interval SF1 the lowest plasticity, greatest stiffness and accompanying greatest resistance to shear deformations thus, favorable conditions for hydraulic fracturing are localized within the belt extending from NE to SW in object covered with seismic survey. Having in mind the location of areas of

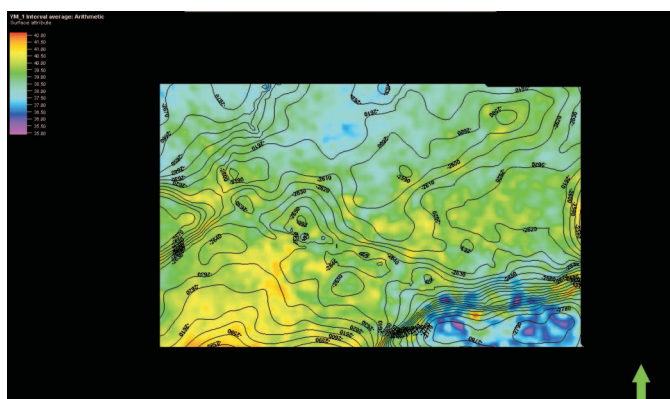


Fig. 1. Map presenting spatial distribution of average values of Young modulus ( $E$ ) in interval SF1 with displayed structure of top of this interval

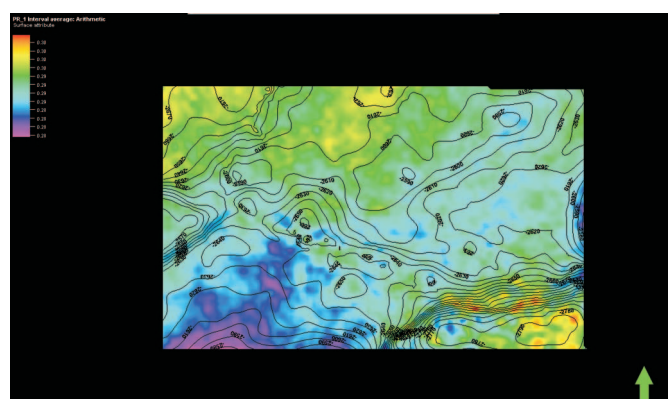


Fig. 2. Map presenting spatial distribution of average values of Poisson's ratio ( $\nu$ ) in interval SF1 with displayed structure of top of this interval

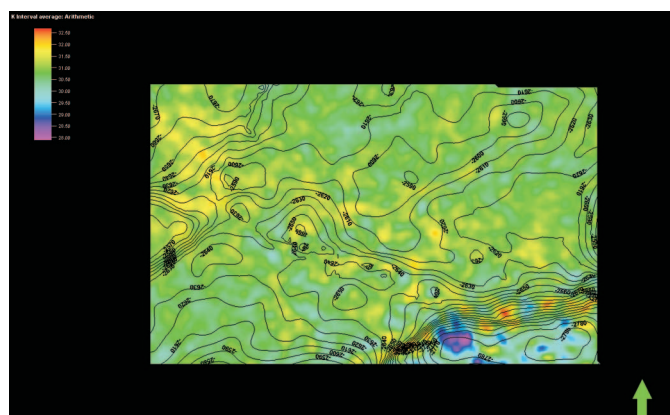


Fig. 3. Map presenting spatial distribution of average values of bulk modulus ( $K$ ) in interval SF1 with displayed structure of top of this interval

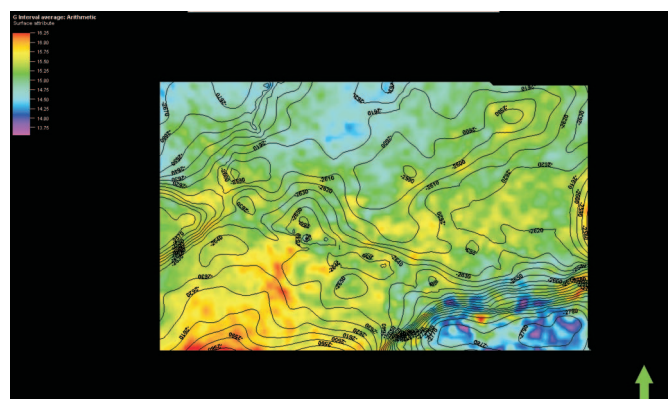


Fig. 4. Map presenting spatial distribution of average values of shear modulus ( $G$ ) in interval SF1 with displayed structure of top of this interval

higher hydrocarbons potential – higher total organic carbon content, this procedure allows for aware selection of zones

that will give satisfactory result of stimulation treatment such as hydraulic fracturing.

### Static and dynamic elastic parameters

The values of elastic parameters show differences depending on the method of measurement. This phenomenon must be taken into account particularly in the case of the use of elastic parameters to build a mechanical model in order to conduct further analysis. Empirically observed difference between the static and dynamic elastic properties (or registered acoustic velocities) can be explained by the difference in the frequency and amplitude of strain applied during measurements of these parameters in static and dynamic conditions [8].

Elastic parameters are commonly calculated from recorded velocity of seismic waves in geologic formation. It is well known that in dispersive medium, the velocity of seismic waves propagation is frequency dependent. Thus, recorded in higher frequencies wave velocity are greater, which directly affects the value of calculated elastic properties. Among methods commonly used to determine elastic properties, the highest frequency of acoustic waves reaching approximately 10 MHz is used during ultra-sonic measurement carried in the laboratory conditions on the rock core or cuttings. The frequency of waves recorded during acoustic logging in the borehole is ~10 kHz, while the frequency of seismic waves during typical seismic survey of geological medium is within range of 10÷50 Hz. With the lowest frequencies we are dealing during laboratory experiments carried out according to the definition of particular elastic properties in the axial compressive test. Such measurements among all methods used to determine elastic properties measure static elastic parameters.

There are many processes affecting the propagation of seismic waves during the measurement of elastic properties in methods mentioned above. First of all, waves induced during seismic profiling, acoustic profiling in borehole or propagating in rock cuttings during ultra-sonic measurement move

through extremely different volumes of rock [13]. Moreover, the value of strain in response to applied stress during these measurements also varies. The difference in deformation is directly reflected in the difference in the calculated stiffness – material's ability to resist stress induced deformation.

Another factor that may be relevant in described phenomenon is the presence of fluid filling the pore space and existing fractures in the rock. In practice, dispersion of compressional wave ( $v_p$ ) is higher than assumed by Biot's theory. It is believed that it is related to the presence of micro-fractures in the rock matrix. At low frequencies, the pore fluid pressure in these fractures will become even to the pore pressure outside the fractures and in consequence existing fracture network will contribute to the pore space in the Biot's model. On the contrary at higher frequencies, the fluid pressure in the fractures will not be able to follow with the rapidly occurring pore pressure oscillations beyond the fractures. As a result fractured zones will be "sealed" and will not constitute the pore space in Biot's model, assuming pore space connectivity. Filled with liquid "sealed" fractured zones will be almost unyielding. Therefore the effective stiffness of the rock matrix will be higher in higher frequencies [13].

Finally, the difference between static and dynamic elastic moduli values can be linked to heterogeneous microstructure of the rock. It can be expected that the underlying cause of the problem can be behavior at the intergranular contact level, as the concentration of stresses in these areas might exceed the limit of the elastic behavior of the material, even at relatively small magnitude of external stress [5]. This could explain the reason why static and dynamic elastic parameters of homogenous materials like steel reveal similar values without statistically meaningful difference.

### Methods for calculating dynamic from static elastic properties

In conventional methods measuring mechanical properties of rock formation i.e. static elastic parameters and strength properties, the measurement is carried out on rock material – plugs or rock cuttings according to the definition of particular elastic property. These type of methods are measuring static elastic properties and are encumbered with some significant disadvantages. First of all, during uni- or triaxial tests, the rock sample undergoes irreversible deformation and most of the time it damages the sample. What is more, these tests are not only time consuming but also are expensive. As a result

they are performed on limited amount of samples, which in turn make full characterization of mechanical properties difficult or even impossible. The measurement of dynamic elastic properties offers advantages over static ones, especially acoustic logging in the borehole and recording of velocities of seismic waves. In these methods we are dealing with continuous registration of wave velocity in the borehole or volume of rocks on which seismic survey is carried out.

In practice, methods allowing for calculation of static elastic properties with the use of dynamic elastic properties

and axial test results are used. For this purpose commonly statistical tools are used in order to find meaningful relationships between static and dynamic elastic parameters starting with simple linear relationships and ending with sophisticated methods using artificial intelligence [6, 12].

### Presentation of data

As mentioned above, results of conducted experiments consequently show the difference in the values between static and dynamic elastic parameters. In many publications and software solutions correlations of static and dynamic according to lithology are proposed. In case of absence of availability of static measurements results conducted on core material what remains are correlation functions from the literature calculated for specific rock types [3]. This approach should nevertheless be used with great caution, as mechanical characteristics of the rocks, for which correlation functions were developed and published, are very specific to particular regions of the world, what is more they are individual for particular sedimentary basin, where were formed under many specific factors including history of stresses acting on the rocks within specific tectonic setting.

On Figure 5 comparison of static and dynamic Young's modulus for borehole W-1 and W-3 is presented.

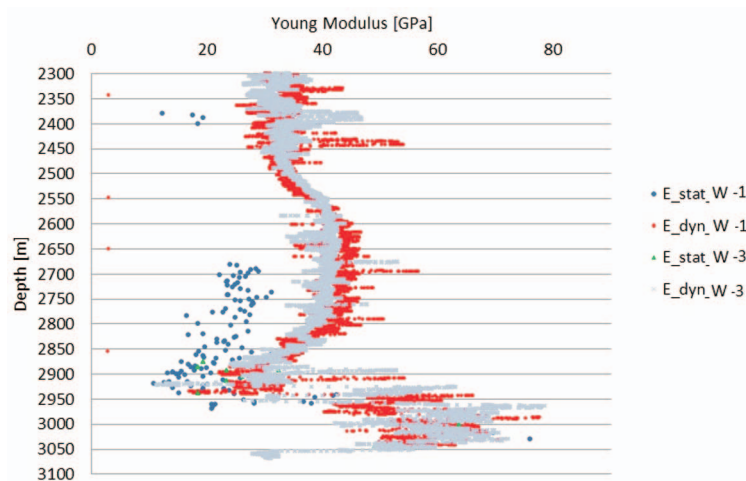


Fig. 5. Static and dynamic Young's modulus measured in the laboratory and registered in W-1 and W-3 boreholes. Dynamic Young's modulus in W-1 borehole is marked in red, while static value of his parameter is marked with blue dots. Dynamic and static Young's modulus in borehole W-1 were marked with purple crosses and green triangles respectively

Dynamic elastic moduli shown in Figure 6 were calculated based on known relations from the literature [5, 7, 8] between velocity of compressional, shear wave and density recorded in the borehole. Static moduli were measured in triaxial tests. As can be seen on Figure 5, the dynamic values of elastic moduli are higher than static ones and the magnitude of this

difference varies. As mentioned above, the cause of the size of the difference between static and dynamic elastic properties can not only change with lithology, but also with fluid saturation and in situ stress state, which can not be accurately reconstructed in the laboratory.

### Correlation functions

For following elastic properties: Young's modulus ( $E$ ), Poisson's ratio ( $\nu$ ), bulk modulus ( $K$ ) and shear modulus ( $G$ ) in selected interval Shale Formation SF1 static and dynamic elastic parameters were compared in order to find linear correlation between these variables (Fig. 6).

All parameters revealed linear correlations with satisfactory correlation coefficients  $R > 0.550$ . The best correlation was obtained for Poisson's ratio with  $R = 0.724$  and the weakest correlation was calculated for bulk modulus with  $R = 0.576$ . Selected interval SF1 was represented by fairly high amount of static measurement results. Among six distinguished intervals of shale formation, there were also intervals poorly represented in which the correlation coefficient were lower, sometimes showing no statistically significant relationship. In case of these poorly represented intervals correlation function was adopted from intervals of most similar lithological characteristics. After application of

linear correlation functions, spatial distributions of elastic properties in the block model were calculated and compared with the distributions of elastic parameters calculated basing on seismic data calibrated with well logs. Spatial distributions of dynamic and corresponding static elastic properties on example of Young modulus obtained with the use of linear correlations are presented on figures 8 and 9. It is worth to mention that according to the author the appropriate spatial distribution of static elastic properties should reflect the distribution of dynamic elastic parameters calculated from seismic data, as in contrast to other methods they continuously describe the entire volume of rock and therefore constitute a good indicator of parameter variability both vertically and horizontally.

As can be seen on enclosed figures, in case of static elastic parameters calculated with the use of linear correlation functions sharp change of values at the transition of particular intervals are noticeable. It is especially visible in case of static Young's modulus at transition of interval SF0 (purple color) and subjected to more detailed characterization in this paper interval SF1 yellowish green) (Fig. 8). This effect is related to uneven sampling of static elastic parameters in the intervals. Intervals poorly represented by static elastic parameters obtained from axial tests were biased due to under- or overestimation. The result

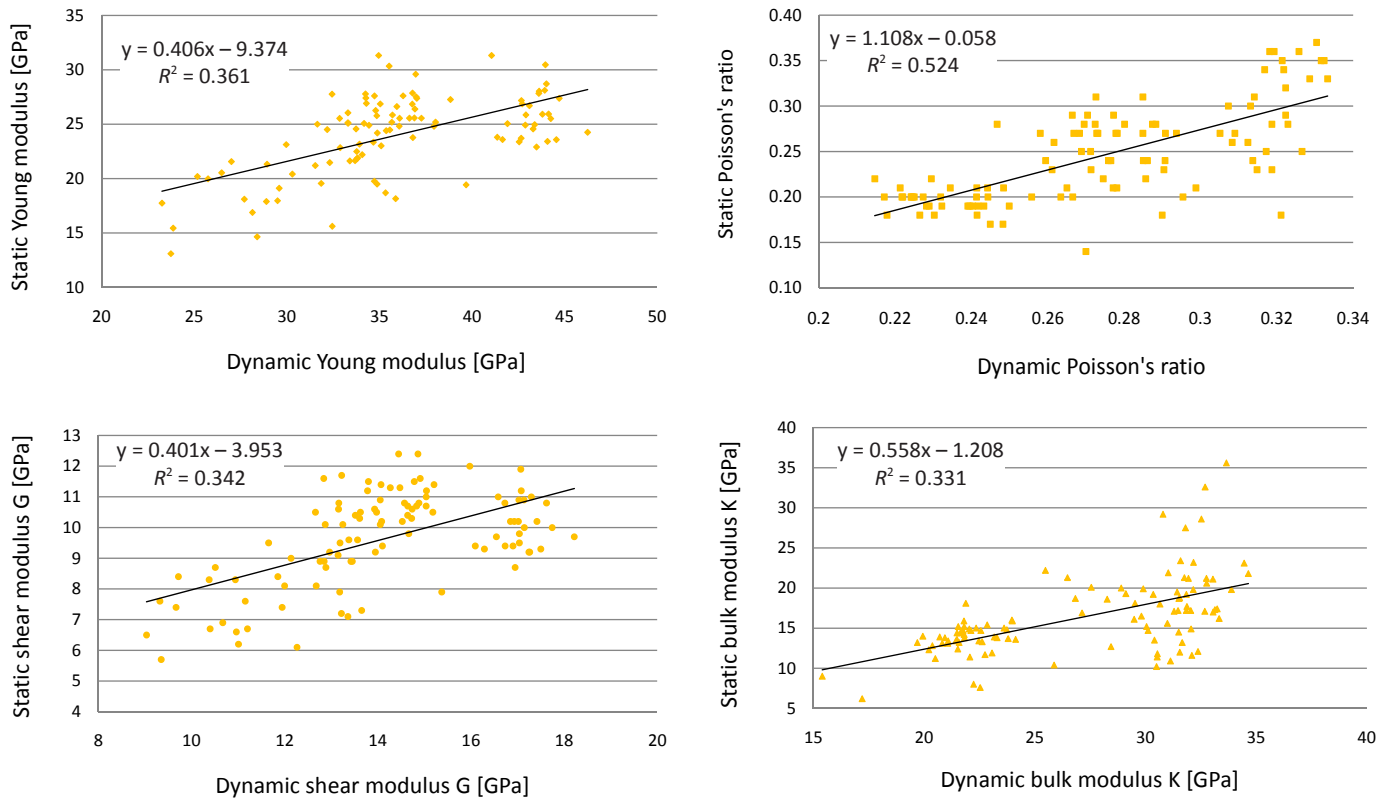


Fig. 6. Static versus dynamic elastic moduli: A – Young’s modulus, B – Poisson’s ratio, C – shear modulus, D – bulk modulus with calculated linear correlation functions and coefficient of determination

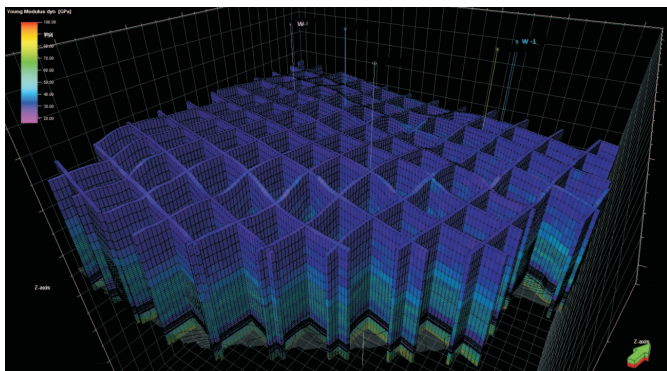


Fig. 7. Fence diagram showing spatial distribution of dynamic Young’s modulus calculated from calibrated with well log seismic data

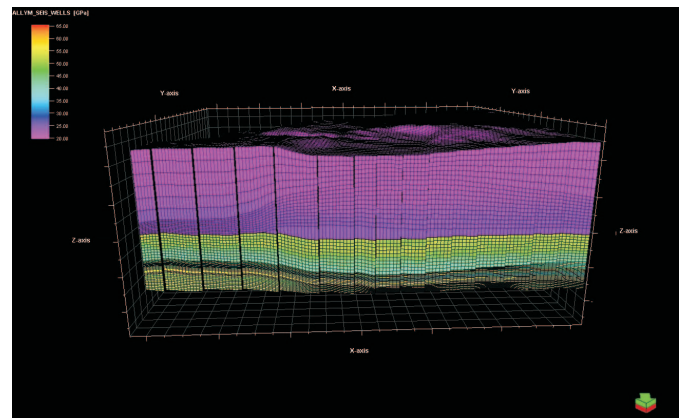


Fig. 8. Spatial distribution of static Young’s modulus obtained with the use of calibrated with well log seismic data and recalculated to static values with the use of linear correlation function

is not satisfactory and does not remind the distribution of elastic parameters occurring in nature.

In order to obtain closer to natural distribution of elastic properties, with regard to distribution calculated from seismic data, more sophisticated method adopting elements of artificial intelligence was used.

**Artificial Neural Networks and Genetic Inversion Algorithm**

Artificial Neural Networks is a branch of artificial intelligence inspired by biological neural networks functionality

of neurons particularly in brain of animals. Artificial neural network is a structure composed of tightly interconnected smaller components (artificial neurons), capable of performing computing processes in parallel. Neural networks have the ability to learn on the basis of available patterns derived from a sufficiently large amount of data sets. At the time of the availability of adequate amounts of sets of data, neural networks seek out relationships and establish patterns between the output and the input dataset. It is a tool used for determining the values

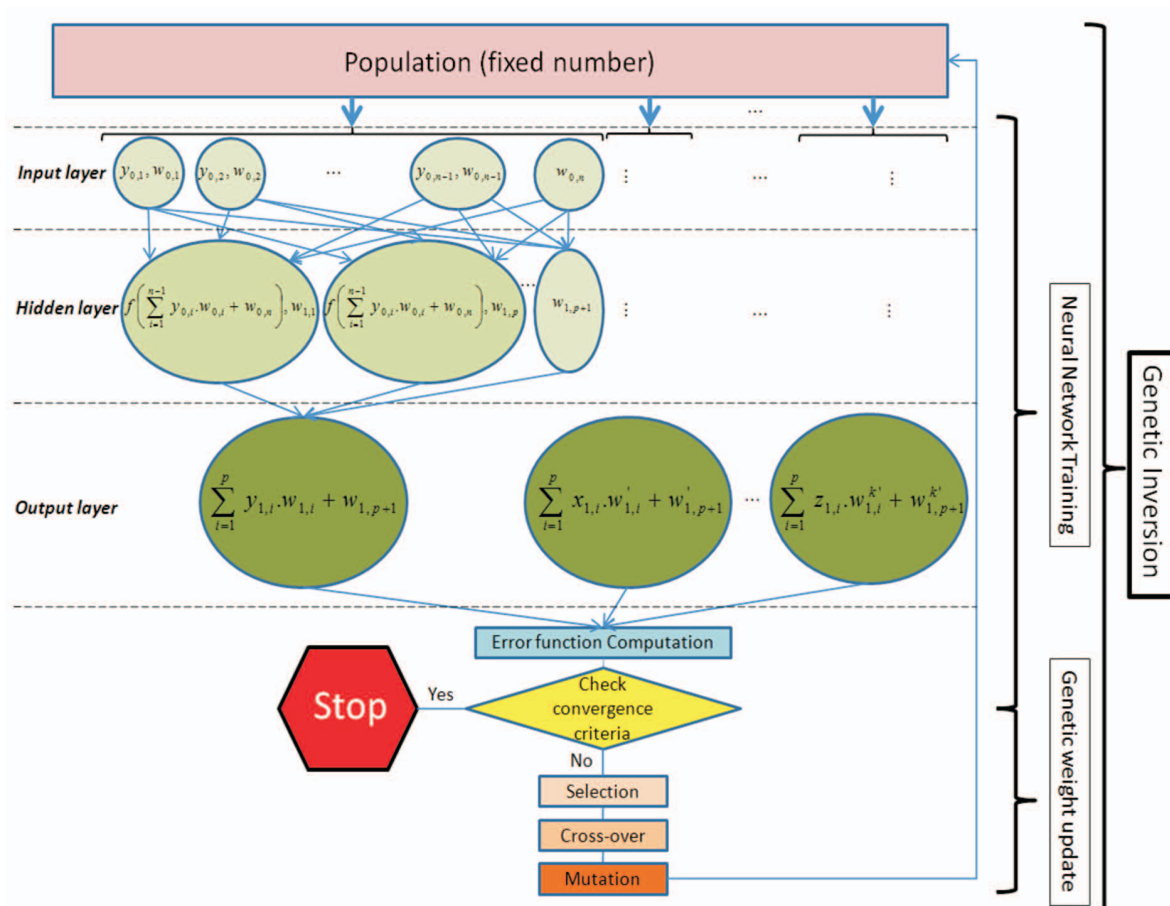


Fig. 9. The genetic algorithm using the elements of Artificial Neural Networks illustrated for input parameters  $x, y$  and  $z$ . Input parameters are used for training of Neural Networks, taking updated by “genetic” part of the algorithm weights via processes of selection, cross-over or mutation [14]

of parameters inherently dependent upon several variables of known value, for example their value was estimated during laboratory measurements. With this tool it is possible to predict a number of wanted parameters, of which measurements is impossible or inviable [12]. Due to wide range of applications, neural networks are a tool becoming more and more popular especially in scientific and engineering disciplines including petroleum geology.

Genetic algorithm combines elements of artificial neural networks, aiming to provide solid result in the form of spatial distribution of the estimated parameter. Imitating phenomena observed in neural cells, genetic algorithm propagates backward to update the error used by the neural network weights. In the described algorithm, to generate the estimation of property, a convergence of this property is forced in such way that the probability of obtaining a minimum global error is much higher than analogous artificial intelligence methods based on the inversion algorithm. Introduction of a Genetic algorithm to Neural Network allowed not only for taking convergence risk into account but also the computation time aspect [14]. Genetic inversion can be used to predict parameters which are directly or indirectly related to the amplitude of seismic

waves, as well as estimate attributes derived from it i.e. density, velocity, porosity and elastic moduli.

The idea of Genetic Inversion algorithm work is presented in Fig. 9. In initial phase of the algorithm sample population (input data) pass through the first iteration of neural networks learning step. The result then is compared with the input data

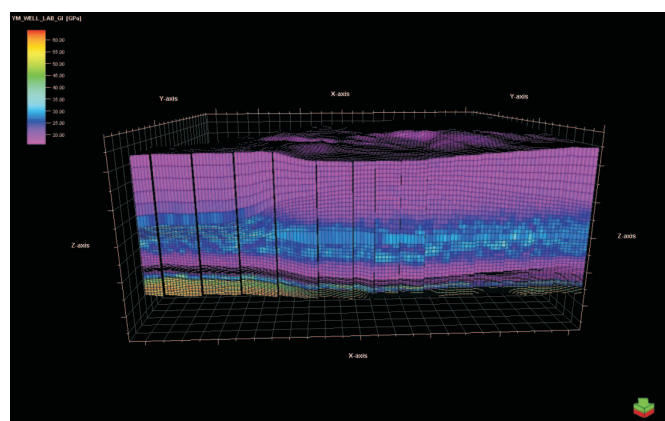


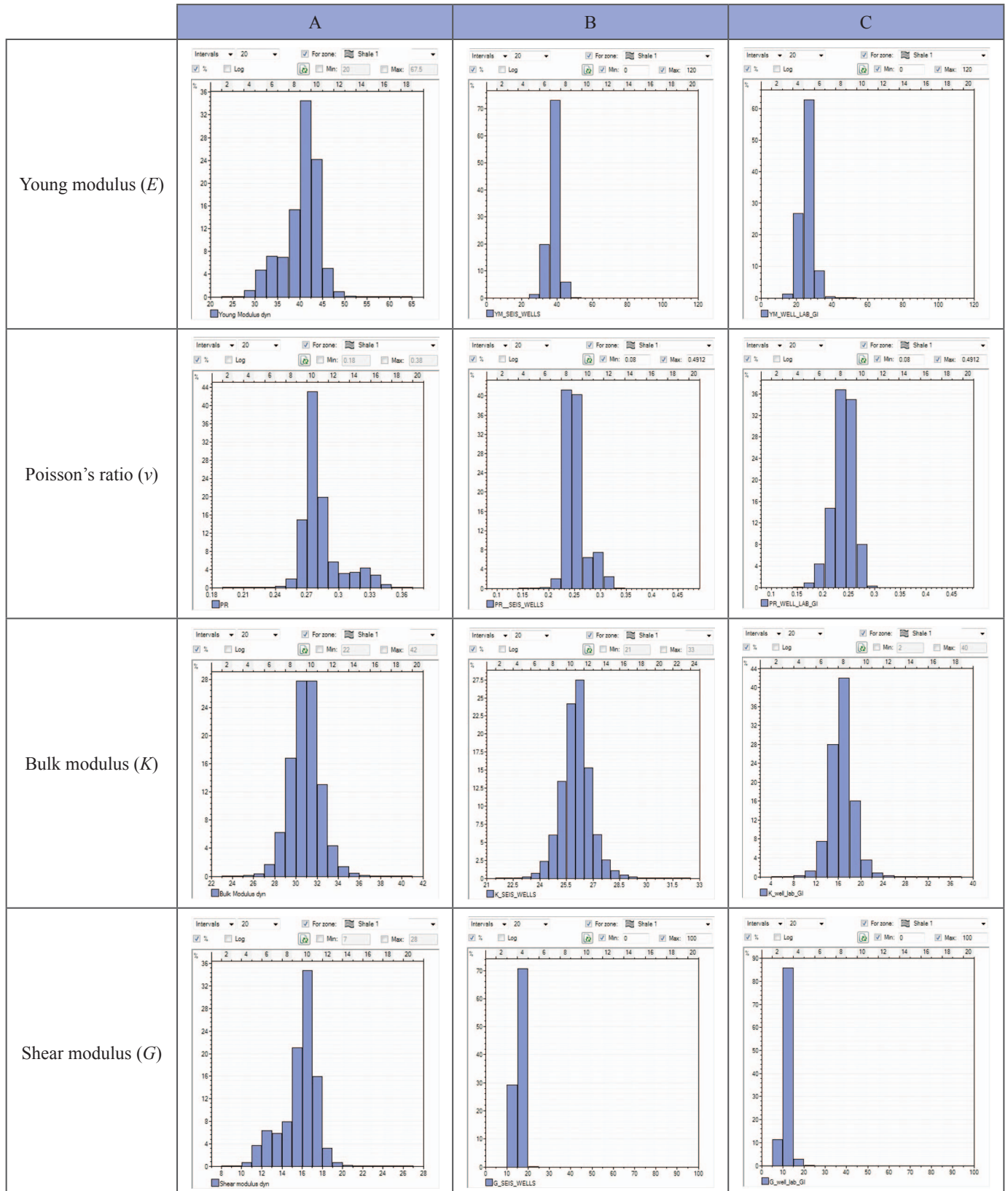
Fig. 10. Spatial distribution of static Young’s modulus obtained with the use of Artificial Intelligence method with calibrated with well log seismic data and static Young modulus as input data



by calculating an error function. At the end of the first iteration performed by Neural Networks, data are captured by the “genetic” part of the algorithm. In genetic inversion algorithm

there are used 3 processes of which the idea is based on the mechanisms that drive biodiversity through the evolution of living organisms. These are: selection, crossing-over and mutation.

Table 2. Distributions of elastic parameters calculated for the Shale Formation SF1 interval based on seismic data (column A), calibrated with well logs seismic data (column B) and calibrated with well logs seismic data and recalculated based on static elastic parameters (column C)



Selection process favors the units that are best adapted to current conditions. In case of genetic inversion the best adaptation means the combination with the smallest error.

Crossing-over is another process derived from biology science, but this time from genetics. During this process, the combination of weighs (“chromosomes”) exchange particular weighs (“genes”) with one another. The process takes place with a given degree of probability during and after each iteration.

Mutation is a process imitating observed in chromosomes sudden change within a gene or chromosome of an organism. This process is intended to minimize converge to a local minimum. The probability of mutation is higher when the error function reaches its plateau. However, the probability of mutation occurrence is much lower than for instance crossing-over process.

The result of described above procedure is a non-linear operator which is used in transformation of seismic volume into estimated property described by input data used at the stage of Neural Network learning.

As a result of genetic algorithm including elements of Neural Networks seismic cubes of static elastic parameters were obtained. The input data were seismic volumes of particular dynamic elastic properties i.e. Young modulus ( $E$ ), Poisson ration ( $\nu$ ), bulk modulus ( $K$ ) and shear modulus ( $G$ ), while data set used for training of Neural Networks in the algorithm were the results of axial tests. The distribution of estimated static elastic property on the example of Young modulus ( $E$ ), is presented on Fig. 10.

Smoother transition of static elastic properties at the interval change are observed. The results obtained with the use of Genetic Inversion algorithm remind more of real distribution that can be seen on Fig. 8 were spatial distribution of dynamic parameters based on calibrated with well log seismic data were presented.

The following Table 2 presents histograms showing the distributions of particular elastic parameters including Poisson’s ratio ( $\nu$ ), Young’s modulus ( $E$ ), shear modulus ( $G$ ) and bulk modulus ( $K$ ) calculated on the basis of seismic data (column A), seismic data calibrated with well log (column B) and seismic data after well log calibration and recalculation with the use of static elastic parameters (column C).

In enclosed Table 2 on histograms of all elastic parameters, with the exception of the distribution of Poisson ratio, a significant shift in the distribution mean towards lower values of elastic parameters manifests. Approximately, static parameters have the value 1.5 (1.4, 1.6 and 1.8 for shear modulus ( $G$ ), Young’s modulus ( $E$ ) and bulk modulus ( $K$ ) respectively) times lower than in comparison with dynamic elastic parameters calculated on the basis of seismic data.

In case of the distribution of Poisson’s ratio ( $\nu$ ), no clear relationship between the increase in Poisson’s ration with increasing frequency was noticed. In addition, for distribution of dynamic elastic parameters no evident difference between dynamic elastic properties calculated from seismic data performed at lower frequencies and dynamic properties calculated based on well logs was observed. If such a difference exists, it is very subtle and was difficult to detect in the characterized interval Shale Formation SF1.

## Conclusions

1. Elastic parameters are one of the basic criteria that should be taken into account when determining the area which is planned to be subjected to hydraulic fracturing.
2. Elastic parameters can be determined during measurements in static conditions and calculated based on measured density and recorded velocity of compressional and shear waves in the borehole or during seismic survey.
3. Due to the nature of available methods, it is possible to distinguish two kinds of elastic properties: static, which are lower in value, and dynamic, that are generally higher.
4. Among presented methods for calculating dynamic to static elastic properties i.e. linear regression and genetic algorithm, better performance was achieved with the use of algorithm based on artificial intelligence (genetic algorithm involving elements of neural networks).

## Summary

In the study analysis of the Lower Paleozoic shale formation was presented. Based on triaxial tests results, well log and seismic data characteristics of elastic properties of the reservoir rock was performed and zones more susceptible to hydraulic fracturing determined.

Also a difference between static and dynamic elastic parameters, its physical cause were presented well as

methodology for conversion of dynamic parameters of more continuous and wider coverage character to static elastic parameters.

The analysis presented in the work is an example of mechanical characterization of shale formation, which requires better recognition for the design of successful hydraulic fracturing treatment.

## Acknowledgments

The Author thank Schlumberger company for providing the software used in this study.

Please cite as: Nafta-Gaz 2015, no. 11, pp. 816–826, DOI: 10.18668/NG2015.11.02

Article contributed to the Editor 31.08.2015. Approved for publication 1.10.2015.

The article is the result of research conducted in connection with the project: *The methodology for determining sweet spots on the basis of geochemical, petrophysical, geomechanical properties based on the correlation of laboratory test results with geophysical measurements and 3D generating model*, co-funded by the National Centre for Research and Development as part of the programme BLUE GAS – POLISH SHALE GAS. Contract No. BG1/MWSSSG/13.

## Literature

- [1] Akbar Ali A. H., Brown T., Delgado R., Lee D., Plumb D., Smirnov N., Marsden R., Prado-Velarde E., Ramsey L., Sponsor D., Stone T., Stouffer T.: *Watching Rocks Change-Mechanical Earth Modeling*. Oilfield Review 2008, pp. 22–39.
- [2] Bjørlykke K., Høeg K., Haque Mondol M.: *Introduction to Geomechanics: Stress and Strain in Sedimentary Basins*. Petroleum Geoscience: From sedimentary Environments to Rock Physics 2010, pp. 281–298.
- [3] Butel N., Hossack A., Kizil M.: *Prediction of in situ rock strength using sonic velocity*. Extended abstracts from 14th Coal Operators' Conference, University of Wollongong, The Australasian Institute of Mining and Metallurgy & Mine Managers Association of Australia, 12–14 February 2014, pp. 89–102.
- [4] Ciechanowska M., Matyasik I., Such P., Kasza P., Lubas J.: *Uwarunkowania rozwoju wydobycia gazu z polskich formacji lupkowych*. Nafta-Gaz 2013, no. 1, pp. 7–17.
- [5] Fjær E., Holt R. M., Horsrud P., Raaen A. M., Risnes R.: *Petroleum Related Rock Mechanics*. 2nd Ed. Elsevier 2008.
- [6] Herwanger J., Koutsabeloulis N.: *Seismic Geomechanics: How to Build and Calibrate Geomechanical Models using 3D and 4D Seismic Data*. EAGE Publications 2011.
- [7] Jędrzejowska-Tyczkowska H., Słota-Valim M.: *Mechaniczny Model Ziemi – jako nowy i konieczny warunek sukcesu w poszukiwaniach i eksploatacji złóż niekonwencjonalnych*. Nafta-Gaz 2012, no. 6, pp. 329–340.
- [8] Mashinsky E. I.: *Differences between static and dynamic elastic moduli of rocks: Physical causes*. Russian Geology and Geophysics 2003, vol. 44, no. 9, pp. 953–959.
- [9] Plumb R., Edwards S., Pidcock G., Lee D., Stacey B.: *The Mechanical Earth Model Concept and Its Application to High-Risk Well Construction Projects Schlumberger*. IADC/SPE Drilling Conference, New Orleans, Louisiana 23–25 February 2000.
- [10] Sayers C.: *Geophysics under stress: geomechanical applications of seismic and borehole acoustic waves: Distinguished Instructor Short Course*. SEG & EAGE 2010.
- [11] Slatt R. M.: *Important geological properties of unconventional resource shales*. Central European Journal of Geosciences December 2011, vol. 3, issue 4, pp. 435–448.
- [12] Sonmez H., Gokceoglu C., Nefeslioglu H. A., Kayabasi A.: *Estimation of Rock Modulus: For Intact Rocks with an Artificial Neural Network and for Rock Masses with the new empirical equation*. Rock Mechanics and Mining Sciences 2006, vol. 43, pp. 224–235.
- [13] Zoback M. D.: *Reservoir Geomechanics*. Cambridge University Press 2010.

## Other used materials

- [14] Schlumberger training materials.



Małgorzata SŁOTA-VALIM M.Sc. Eng.  
Junior Scientist  
Department of Geology and Geochemistry Laboratory of Petrophysics  
Oil and Gas Institute – National Research Institute  
ul. Lubicz 25 A, 31-503 Kraków  
E-mail: slota@inig.pl